Research Square

Preprints are preliminary reports that have not undergone peer review.
They should not be considered conclusive, used to inform clinical practice,
or referenced by the media as validated information.

Dual wavelengths along with dark pulse mode-locked fiber laser generation using Polyaniline Boron Nitride Nanocomposite as saturable absorber

Hasanain Naser Abd Ali

hn.nr.aa@gmail.com

Technical University of Malaysia Malacca

Anas Abdul Latiff

Technical University of Malaysia Malacca

Aeriyn D. Ahmad

University of Malaya

Sulaiman Wadi Harun

University of Malaya

Research Article

Keywords: Polyacrylonitrile, Boron Nitride, Mode-locked, saturable absorber, Erbium, Fiber Laser.

Posted Date: May 20th, 2026

DOI: https://doi.org/10.21203/rs.3.rs-8981581/v1

License: This work is licensed under a Creative Commons Attribution 4.0 International License.
Read Full License

Additional Declarations: No competing interests reported.

Version of Record: A version of this preprint was published at Journal of Materials Science: Materials in Electronics on July 4th, 2026. See the published version at https://doi.org/10.1007/s10854-026-17881-x.

Dual wavelengths along with dark pulse mode-locked fiber laser generation using Polyaniline Boron Nitride Nanocomposite as saturable absorber

Hasanain Naser Abd Ali[1*], Anas Abdul Latiff[1*], Aeriyn D. Ahmad[2], Sulaiman Wadi Harun[2]

[1] Fakulti Teknologi dan Kejuruteraan Elektronik dan Komputer (FTKEK), Universiti Teknikal Malaysia Melaka (UTeM), 76100, Hang Tuah Jaya, Durian Tunggal, Melaka, Malaysia.

[2] Photonics Engineering Laboratory, Department of Electrical Engineering, University of Malaya, 50603 Kuala Lumpur, Malaysia.

Corresponding authors: hn.nr.nr@gmail.com & anasabdullatiff@utem.edu.my

Abstract

A dual-wavelength fiber laser exhibiting mode-locked dark pulse production is shown, using Polyaniline Boron Nitride Nanocomposite (PANI-BN) as a saturable absorber (SA). The integration of PANI-BN, a nanocomposite, allows the production of stable mode-locked dark pulses at dual synchronous wavelengths of 1532.4 nm and 1557.2 nm, exhibiting a spectral separation of 24.8 nm. The dual-wavelength functioning results from the nonlinear effects in the PANI-BN nanocomposite, which displays unique optical features that enable effective pulse production at these wavelengths. The system functions with an adjustable input pump power range of 129.9 mW to 212.1 mW. The repetition rate of the produced pulses stays consistent at 1.225 MHz while the pump power is adjusted, which is a crucial attribute for applications necessitating great temporal accuracy. The pulse width, an essential parameter for pulse shaping, fluctuates between 559 ns and 502 ns, contingent upon the pump power. The fluctuation in pulse width elucidates the dynamics of the laser under varying operational settings, demonstrating the effective interaction of the PANI-BN nanocomposite as a saturable absorber. The pulse energy produced by the laser system fluctuates between a high of 1140.9 nJ and a low of 216.3 nJ, with the average output power ranging from 1.1 mW to 5.8 mW. The numbers indicate the effective energy conversion inside the system, with the maximum pulse energy being especially important for high-power applications. The slope efficiency of the fiber laser is recorded at 6.16%, indicating a modest but consistent efficacy in transforming pump power into useable laser output. This fiber laser's dual-wavelength characteristic, including a significant 24.8 nm separation, along with steady mode-locked dark pulse production, facilitates diverse applications such as high-resolution spectroscopy, optical communications, and sensing. The findings indicate that PANI-BN nanocomposites serve as a viable alternative optical modulator for pulsed fiber laser applications. This study emphasizes the promise of using innovative nanocomposite materials such as PANI-BN to enhance the efficacy and adaptability of fiber laser systems, facilitating the development of more compact, efficient, and versatile fiber laser sources for many scientific and industrial applications.

Keywords

Polyacrylonitrile, Boron Nitride, Mode-locked, saturable absorber, Erbium, Fiber Laser.

1. Introduction

Fiber lasers functioning in the 1.5 μm wavelength range have garnered considerable interest due to their intrinsic benefits, such as superior beam quality, compact design, high efficiency, and compatibility with conventional telecommunication components [1]. This spectral window is crucial as it aligns with the low-loss and low-dispersion transmission window of silica optical fibers, rendering fiber lasers exceptionally appropriate for optical communications, sensing, biomedical diagnostics, nonlinear optics, and ultrafast photonics applications [2]. In erbium-doped fiber laser (EDFL) systems, laser oscillation is attained via population inversion in Er^{3+} ions, with the emitted wavelengths and pulse characteristics determined by the interplay of gain bandwidth, cavity dispersion, nonlinear optical phenomena, and intracavity elements [3]. Through meticulous design of the fiber laser cavities, including the choice of gain fiber length, dispersion control, and nonlinear components, many pulse regimes including continuous-wave, Q-switched, and mode-locked operation may be achieved [4, 5]. Specifically, passive mode-locking facilitates the production of stable ultrafast pulses by imposing phase coherence across longitudinal cavity modes via an intensity-dependent loss process [6].

The selection of a saturable absorber is essential in influencing the pulse dynamics and stability of mode-locked fiber lasers [7]. Composite and hybrid materials have recently attracted significant attention as saturable absorbers owing to their improved nonlinear optical responses resulting from synergistic interactions among their constituent materials [8]. Polyaniline (PANI) is a conductive polymer recognized for its adjustable electrical conductivity, chemical stability, environmental resilience, and significant nonlinear optical absorption [9]. PANI has rapid carrier dynamics and extensive absorption properties, making it a compelling option for passive pulse production in fiber laser systems [10]. Boron nitride (BN), especially in its hexagonal configuration, is a wide-bandgap substance noted for its elevated heat conductivity, superior mechanical strength, and optical transparency throughout an extensive spectrum range [11]. When integrated with PANI to create a nanocomposite, BN may augment thermal dissipation, promote material stability, and alter the nonlinear optical response of the composite, hence optimizing the efficacy of the saturable absorber under elevated optical intensities [12].

Dual-wavelength fiber lasers constitute a significant category of laser sources owing to their extensive applications in optical beating generation, wavelength-division multiplexing, microwave photonics, sensing, and spectroscopy [13]. Dual-wavelength functioning in fiber lasers may be accomplished by many methods, such as gain competition, cavity birefringence, wavelength-selective filtering, and nonlinear phenomena [14]. The introduction of passive mode-locking in such systems might result in the coexistence of two lasing wavelengths, leading to intricate pulse dynamics, including synchronous pulse creation at multiple wavelengths [15, 16]. Dark pulse mode-locking, distinguished by localized intensity dips on a continuous-wave background, has garnered significant interest due to its distinctive physical properties and potential benefits, including increased robustness against disturbances and reduced peak power relative to bright pulses [17]. Dark pulses often arise in fiber laser cavities characterized by predominant normal dispersion, with their emergence dictated by the equilibrium among dispersion, nonlinearity, gain, and saturable absorption [18, 19].

The use of a PANI–BN nanocomposite saturable absorber into a fiber laser cavity provides an advantageous framework for achieving dual-wavelength mode-locked dark pulse operation [20]. The nonlinear absorption of the PANI–BN composite facilitates intensity-dependent loss modulation, promoting stable mode-locking, while the composite structure presents wavelength-dependent absorption and loss characteristics that enable simultaneous

oscillation of multiple wavelengths [21]. The interplay of cavity birefringence, gain competition in the erbium-doped fiber, and the nonlinear response of the PANI–BN saturable absorber facilitates the emergence of dual-wavelength operation with dark pulse dynamics [22]. The enhanced thermal stability and mechanical strength afforded by BN further boost long-term operational stability, which is crucial for sustaining sustained dark pulse mode-locking [23, 24].

This study experimentally demonstrates a dual-wavelength mode-locked dark pulse fiber laser functioning using a polyaniline–boron nitride nanocomposite as a saturable absorber. The laser concurrently produces two stable wavelengths at 1532.4 nm and 1557.2 nm, validating the efficacy of the PANI–BN nanocomposite in facilitating intricate pulse dynamics inside a fiber laser cavity. The successful implementation of dual-wavelength dark pulse mode-locking underscores the significant potential of PANI–BN nanocomposites as sophisticated saturable absorbers for next-generation fiber laser systems, therefore broadening their utility in ultrafast photonics and multi-wavelength laser technologies.

2. Fabrication and characterization of the Polyaniline Boron Nitride (PANI-BN) as a SA.

The thin-film saturable absorber (SA) was produced by a solution-casting method, wherein commercially available PANI–BN powder was incorporated into an acrylic polymer solution, namely Polymethyl Methacrylate (PMMA) and commonly known as acrylic or acrylic glass. PMMA was chosen as the host matrix because to its superior optical clarity, exceptional chemical and thermal stability, consistent film-forming capabilities, and significant mechanical strength and flexibility. The advantageous characteristics of PMMA render it an optimal medium for attaining uniform dispersion of PANI–BN particles, thereby guaranteeing dependable and efficient saturable absorption performance.

During the manufacturing procedure, 5 mL of the produced PMMA solution was put into an analytical glass vial containing 2 mg of PANI–BN powder, which was precisely weighed using a high-precision balance. The mixture was constantly agitated for around 72 hours to ensure full dissolution and uniform dispersion of the PANI–BN particles inside the PMMA matrix, as seen in Fig. 1. After achieving a homogenous solution, the mixture was transferred to a 6 cm diameter Petri dish for film creation. The solvent was let to evaporate spontaneously at ambient temperature for 72 hours, yielding a self-supporting thin film with an average thickness of around 50 μm.

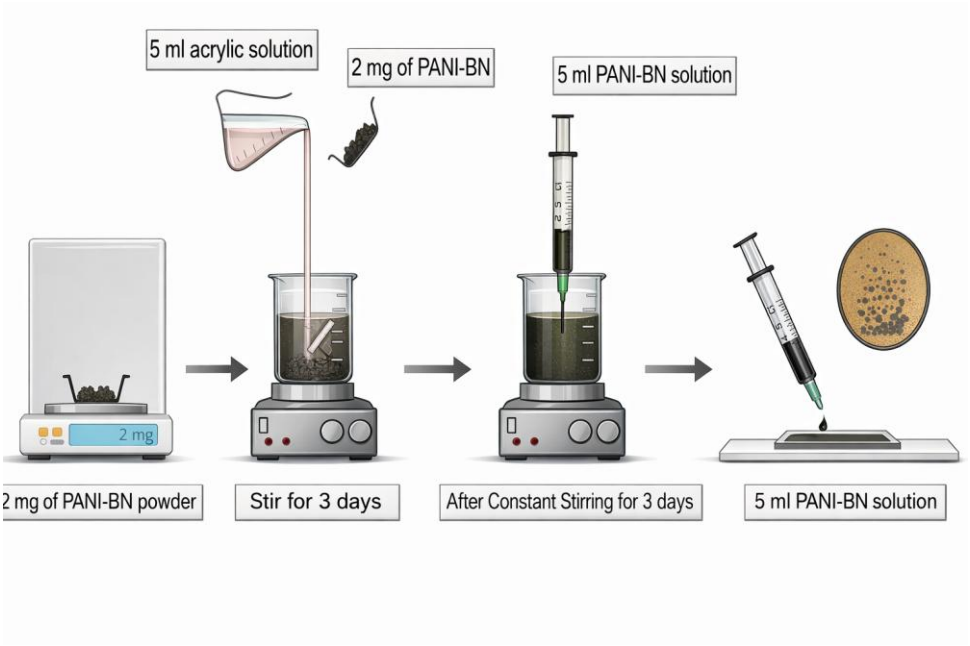


Figure 1: Step by step fabrication process of PANI-BN-acrylic film

The synthesized PANI–BN–acrylic thin film, seen in Fig. 2(a), exhibits a straightforward production method and may be easily incorporated into erbium-doped fiber laser (EDFL) cavities. Field-emission scanning electron microscopy (FESEM) was used to analyze the surface morphology and material distribution inside the composite film. The FESEM pictures validate the effective integration of the PANI–BN nanomaterial into the PMMA host matrix. Fig. 2(b) clearly depicts the saturable absorber situated inside the fiber core area, while Fig. 2(c) demonstrates a random but uniform distribution of PANI–BN particles throughout the polymer matrix, signifying excellent film homogeneity.

An energy-dispersive X-ray spectroscopy (EDS) examination was conducted to examine the elemental composition of the PANI–BN–acrylic thin film. Fig. 2(d) displays the EDS spectrum, which reveals three predominant elements in the composite: carbon (67.01 wt%), oxygen (29.63 wt%), and nitrogen (3.36 wt%). The presence and proportions of these constituents affirm the effective incorporation of the PANI–BN nanocomposite into the PMMA matrix, hence certifying the material composition and structural integrity of the produced saturable absorber.

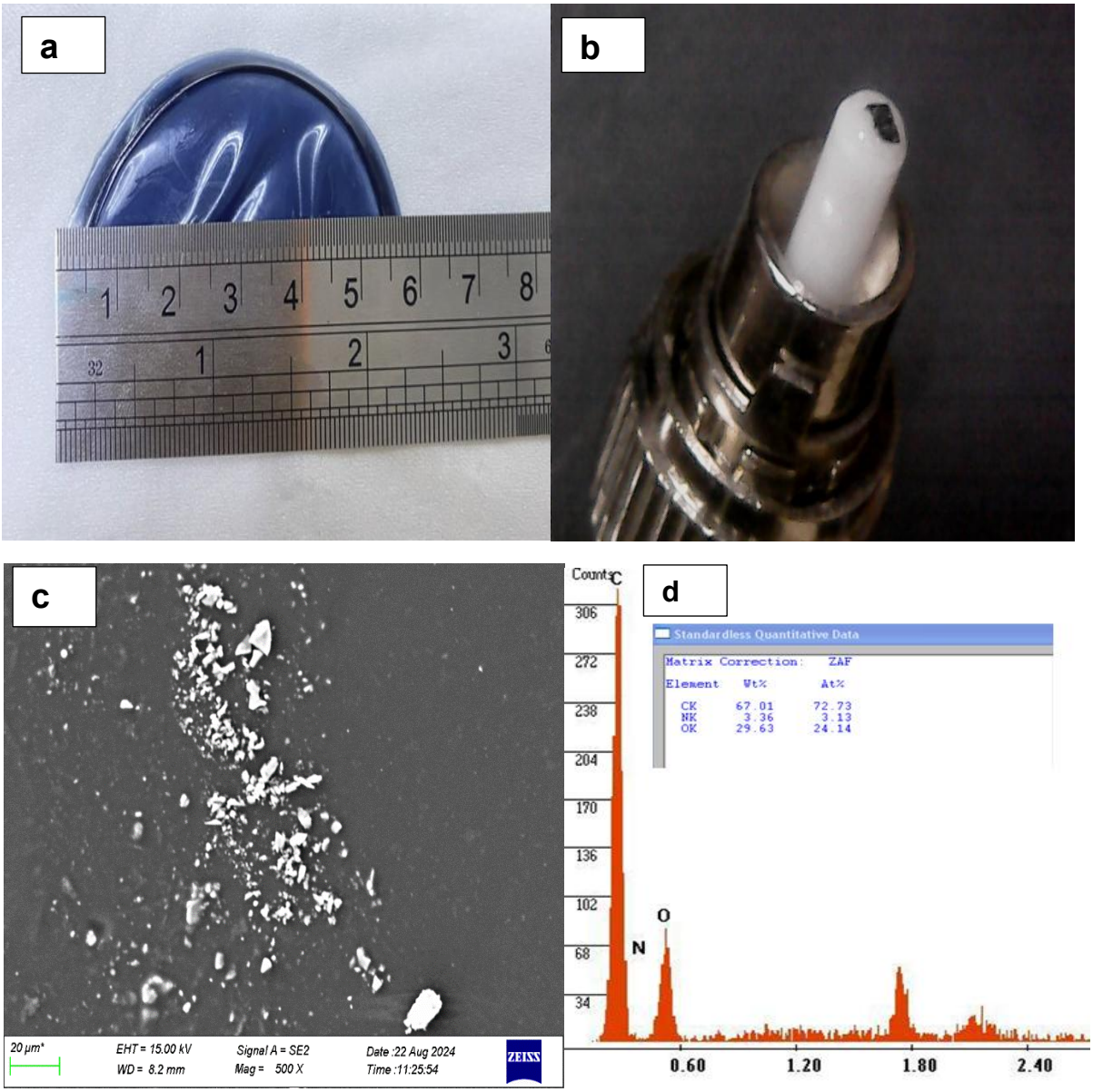


Figure. 2. SA device (a) an image of the PANI-BN thin film, (b) SA location in the patch core (c) its corresponding FESEM image at 500 X Magnification and (d) EDS Result.

3. Laser setup and experimental work

Fig. 3 illustrates the schematic of the C-band mode-locked fiber laser, which includes a two-stage optical amplification system and a PANI–BN-based saturable absorber (SA). The laser cavity was configured in a unidirectional ring arrangement. A dual-stage erbium-doped fiber (EDF) amplifier facilitated optical amplification, with each stage consisting of a 1 m long EDF energized by a laser diode via a couple of wavelength-division multiplexer (WDM). An optical isolator was placed between the two amplification stages to guarantee unidirectional light passage and to eradicate unwanted back reflections. The use of a two-stage amplification framework facilitates the production of amplified spontaneous emission in a quasi-dual-laser setup, crucial for expanding laser functionality into the C-band spectrum. This process involves the partial reabsorption of photons created in the C-band, which contributes to the population inversion necessary for C-band emission, hence improving lasing efficiency in the C-band spectrum.

Passive mode-locking was achieved by incorporating the PANI–BN saturable absorber into the laser cavity. The SA was constructed by encasing the PANI–BN–PVA thin film between two fiber ferrules and securing it with a fiber optic adapter. A 100 m length of standard single-mode fiber (SMF) was integrated into the cavity to provide sufficient dispersion and nonlinear interaction for steady pulse generation. An optical coupler with a 20:80 ratio was used to remove a fraction of the circulating optical power, while the residual light was recirculated inside the cavity to maintain laser oscillation. The total cavity length was around 115 m, yielding a fundamental repetition rate of approximately 1.82 MHz. The polarization controller (PC) inside the fiber laser cavity guarantees the optimal alignment of the light's polarization state for effective interaction with the saturable absorber, facilitating steady mode-locking or Q-switching operation. It facilitates the maintenance of constant pulse production by adjusting the polarization conditions inside the cavity.

The laser's output characteristics were assessed utilizing an optical spectrum analyzer (OSA, Yokogawa AQ6370D), a digital oscilloscope (GWINSTEK GDS-3502), and a radio-frequency spectrum analyzer (RFSA, Anritsu MS2830A) to examine its spectral properties, temporal dynamics, and operational stability. Before being detected by the oscilloscope and RFSA, the optical signal was transformed into an electrical signal using a high-speed photodetector (EOT ET-5000F). The mean output power was further assessed using an optical power meter (Thorlabs PM400) paired with a calibrated power sensor (Thorlabs S405C).

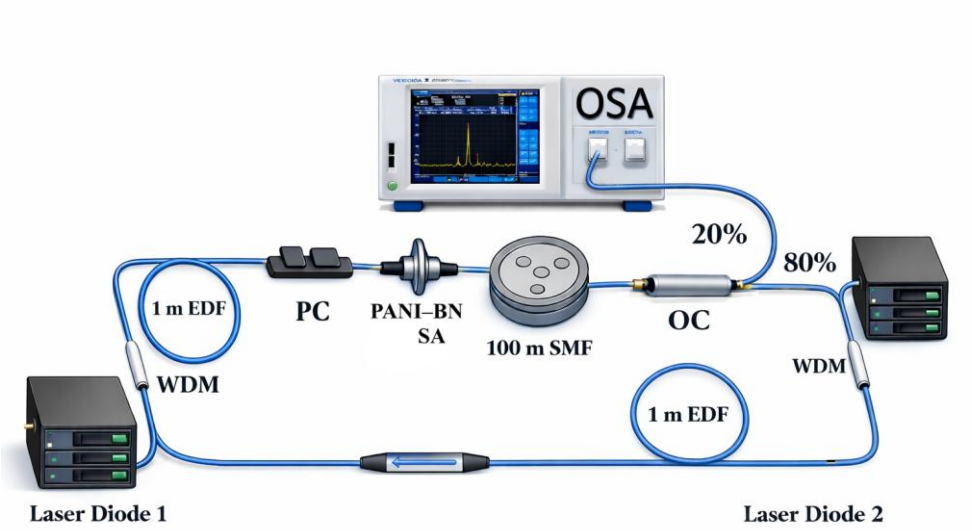


Figure. 3. Configuration of mode-locked EDFL incorporating a two-stage EDF amplifier as the gain medium and the fabricated PANI–BN film as the SA for passive mode-locking

4. Results and discussion

Upon incrementally augmenting the pump power, the first observation of steady mode-locked dark pulse production was recorded. The operational state persisted until the pump power reached 212.1 mW. Beyond this level, the laser seamlessly switched into a steady dark pulse mode-locked functioning. This change signified successful pulse generation inside the cavity. At the onset of mode-locking, the average output power varied between 1.1 mW and 5.8 mW, indicating enough energy accumulation inside the cavity for pulse production. The mode-

locked dark pulse operation exhibited stability despite variations in pump power ranging from 129.9 mW to 212.1 mW, with no indications of pulse disruption or amplitude variations.

The repetition rate (RR) was consistently maintained at 1.225 MHz, demonstrating the robust uniformity of the pulse train. The pulse width (PW) fluctuated between 559 ns and 502 ns with increasing pump power, indicating a reduction in pulse length attributed to higher energy extraction from the gain medium and improved population inversion. Pulse energy (PE) varied from 1140.9 nJ to 216.3 nJ, demonstrating the efficient storage and release of energy in the laser cavity. The findings validate that the dynamics of dark pulses are intricately associated with the pump power level. With the escalation of pump power, the pulse length consistently decreased, aligning with the characteristics of passively mode-locked fiber lasers, whereby the saturable absorber reaches saturation more rapidly, resulting in abbreviated energy release intervals. Exhibits the pulse profile with intervals of 860 ns between pulses, indicating a good level of stability in pulse creation at consistent input power, with no notable fluctuations seen between pulses as shown in fig. 4 (a, b)

The consistency of pulse amplitudes over the whole pump power spectrum further illustrates the efficacy and reproducibility of the mode-locked dark pulse operation. The results indicate that augmenting pump power improves energy storage inside the laser cavity, resulting in elevated repetition rates, reduced pulse widths, and stable pulse intensity. This highlights the dependability and efficacy of the suggested fiber laser configuration.

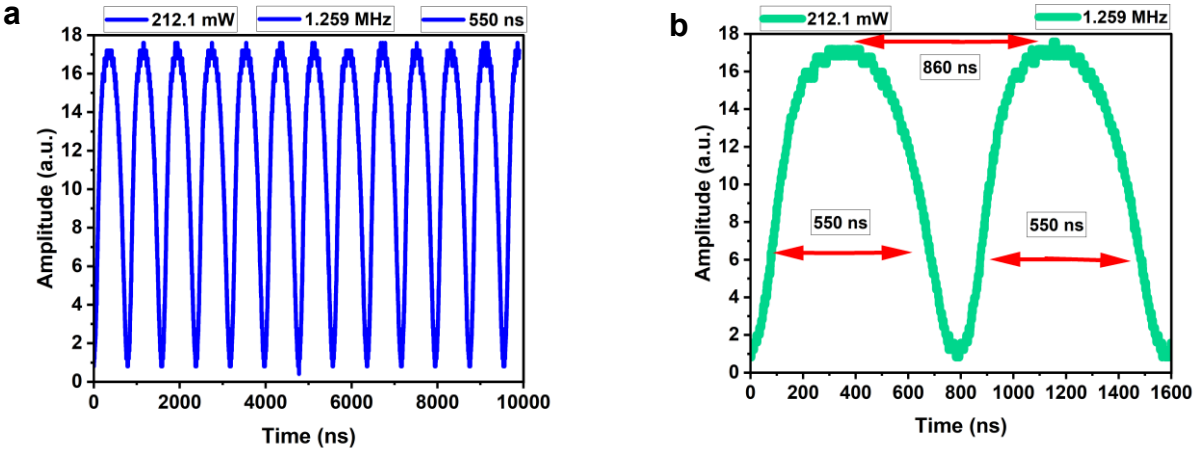


Figure 4. Oscilloscope pulse train at pump power max level 212.1 mW shows: (a) The full Mode-locked, (b) Zoom in pulse to show the pulse width and time periods.

Fig 5. In dual-wavelength operation, the maximum peak is seen at 1557.2 nm, with the laser emitting pulses at two separate wavelengths: 1532.4 nm and 1557.2 nm. The spectral gap between these two wavelengths is 24.8 nm, a crucial aspect of the dual-wavelength operation, which is influenced by nonlinear phenomena inside the laser cavity. This spectral separation demonstrates the effective and accurate pulse production at both wavelengths concurrently, facilitated by the PANI-BN saturable absorber.

Conversely, the continuous-wave (CW) operation is distinguished by a single, larger peak at 1568.1 nm. The change in peak wavelength signifies the distinct operational circumstances of the continuous wave mode in contrast to the dual-wavelength operation, whereby the laser

produces a continuous output devoid of the pulse modulation characteristic of the mode-locked regime.

The comparison of the two spectra clearly illustrates the differences in emission profiles: the continuous wave operation exhibits a single emission peak, while the dual-wavelength operation yields two discrete peaks, therefore validating the successful creation of mode-locked dark pulses at two unique wavelengths. The dual-wavelength phenomenon, characterized by significant spectral separation, provides a distinct benefit for applications necessitating precise wavelength regulation, including high-resolution spectroscopy and optical communications.

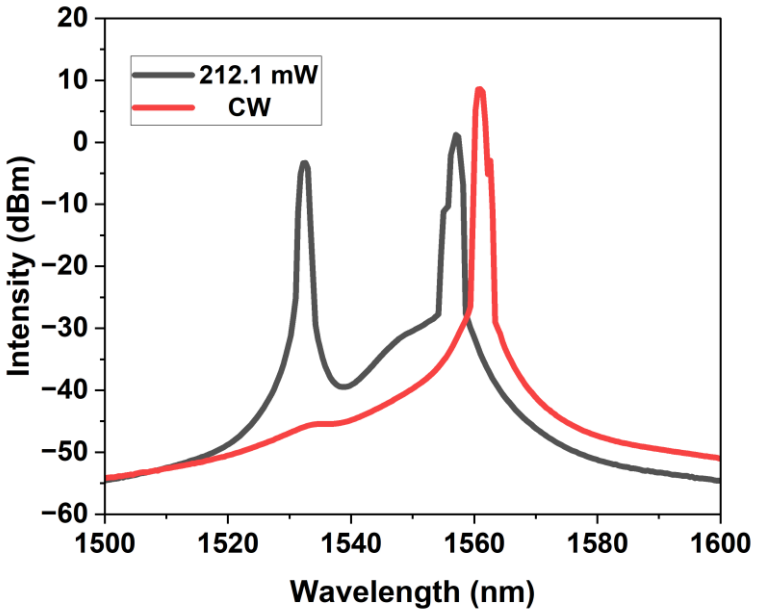


Figure 5. The graph illustrates the intensity spectra for both the dual-wavelength operation and continuous wave (CW) operation of the fiber laser at a pump power of 212.1 mW

Fig. 6. This 3D graph illustrates the spectrum intensity of the fiber laser across varying pump power levels, from 129.9 mW to 212.1 mW. With an increase in input power, the intensity of the dual-wavelength peaks at 1532.4 nm and 1557.2 nm, exhibiting a spectral separation of 24.8 nm, likewise escalates. At the minimal pump power of 129.9 mW, the output power varies between 1.1 mW and 5.8 mW, exhibiting consistent and clearly defined peaks, indicative of excellent performance for dual-wavelength operation.

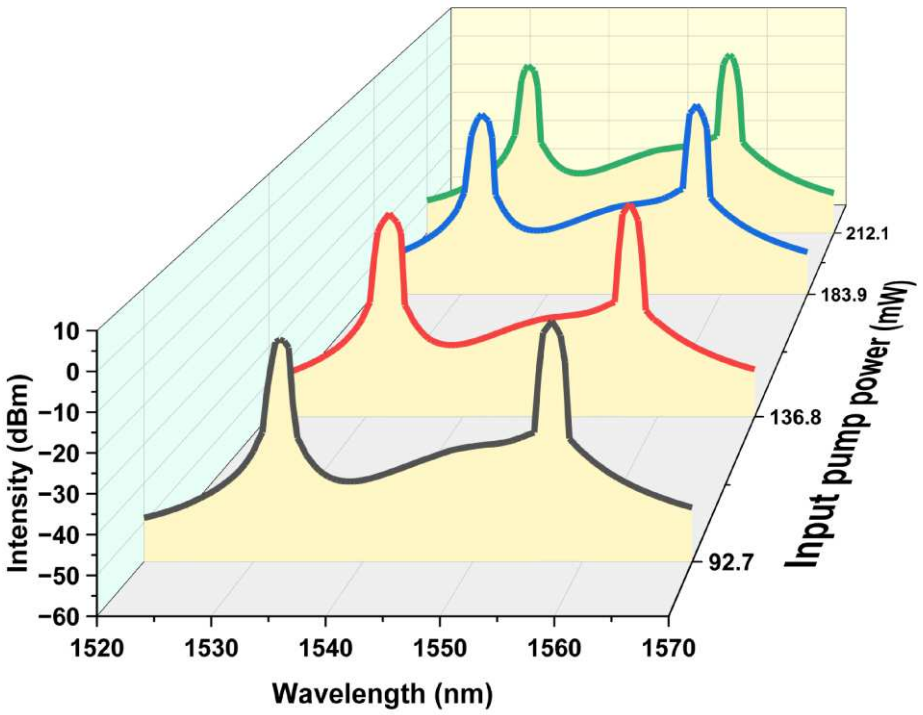


Figure 6. 3D graph displays the spectral intensity of the fiber laser at different pump power levels

To evaluate the durability of maximal dual-wavelength operation over time, optical spectra were acquired every 10 minutes for a continuous duration of one hour. The data shown in Fig. 7. indicate that the spectral properties, including the form, intensity, and bandwidth of the peaks at 1532.4 nm and 1557.2 nm, were stable over the whole time. The spectral separation of 24.8 nm and the intensity levels exhibited little fluctuation, so affirming the consistent performance of the dual-wavelength operation throughout time. This stability is essential for applications necessitating dependable and consistent pulse production, signifying that the laser system maintains stability even after extended operation.

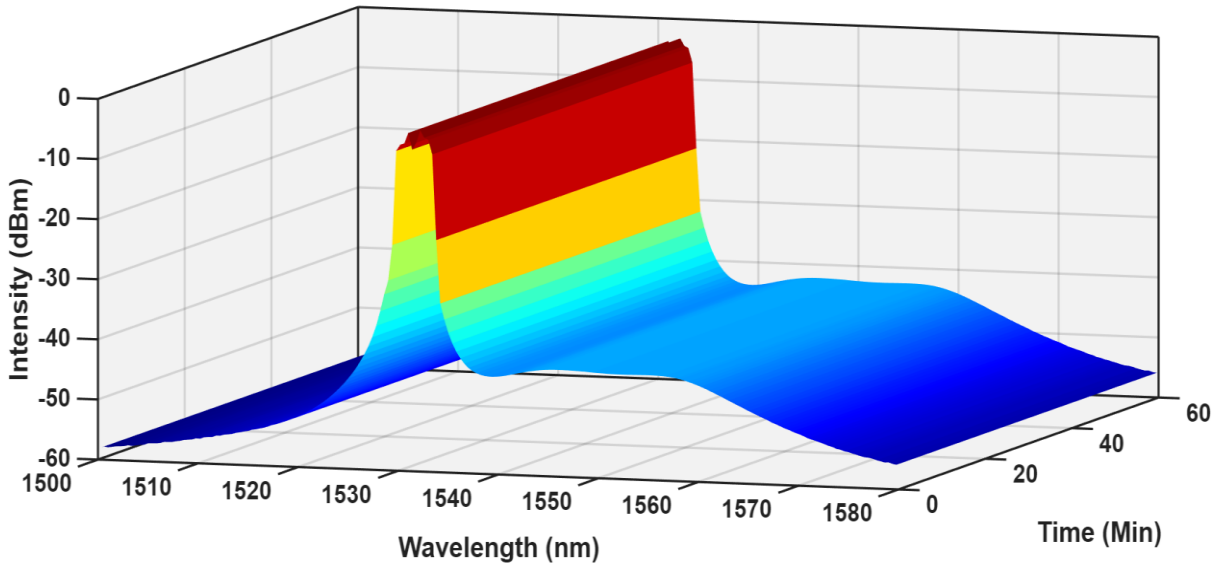


Figure 7. Evaluate the durability of maximal dual-wavelength operation over time

Fig. 8, presents the RF spectrum study of the fiber laser at a peak pump power of 212.1 mW, shown in two plots (a and b). Fig. 8 (a) illustrates an extensive frequency range with a signal-to-noise ratio (SNR) of 70 dB and a primary repetition frequency of around 200 kHz, signifying reliable pulse production with little noise. The several minor peaks in this graph indicate that the system generates reliable pulses devoid of substantial distortion or interference. Fig. 8(b) offers an enlarged perspective of the spectrum, concentrating on the primary peak, where the SNR is maintained at 70 dB, therefore affirming a pristine and noise-free signal. The primary peak is seen at around 150 kHz, so corroborating the reliable pulse creation. The RF spectra indicate that the laser functions with little temporal jitter and good stability, guaranteeing dependable performance even at peak pump power.

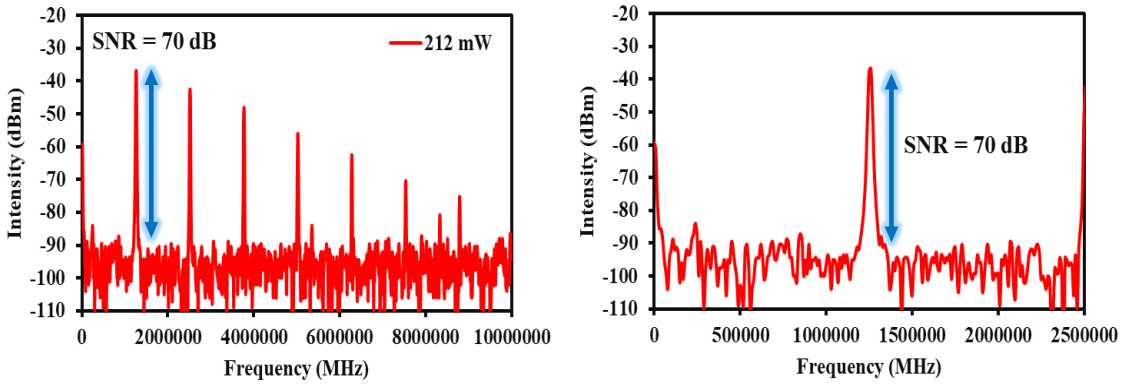


Figure 8. (a, b) shows the radio frequency (RF) spectrum at max pump power of along with the SNR.

Fig. 9, illustrates the correlation among input power, output power, and pulse energy in the dual-wavelength fiber laser system. As shown, an increase in input pump power (from 1 to 10 mW) results in a corresponding rise in both output power and pulse energy. The output power increases from about 1 mW to 5.8 mW, and the pulse energy escalates from 216.3 nJ to 1140.9 nJ with input power from 92.7 mW to 212.1 mW. This linear rise indicates that a greater amount of energy is effectively transformed into useable laser output with rising pump power, leading to enhanced pulse energy and output power. The direct relationship between pulse energy and output power demonstrates the system's efficient conversion of pump energy into laser energy.

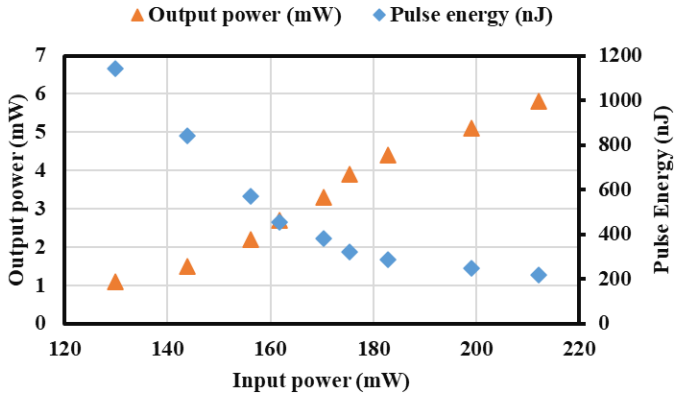


Figure 9. Relationship between input power, output power, and pulse energy, showing linear increase with input power

Fig. 10, Examines the correlation between input power and output power, as well as the system's slope efficiency. As the input power escalates from 129.9 mW to 212.1 mW, the output power consistently rises from 1.1 mW to 5.8 mW. The system's slope efficiency is determined to be 6.16%, indicating a reliable and effective conversion of pump energy into laser output. The steady but moderate slope efficiency indicates that the system operates consistently and efficiently throughout varying input power circumstances, maintaining stable output power over the evaluated range.

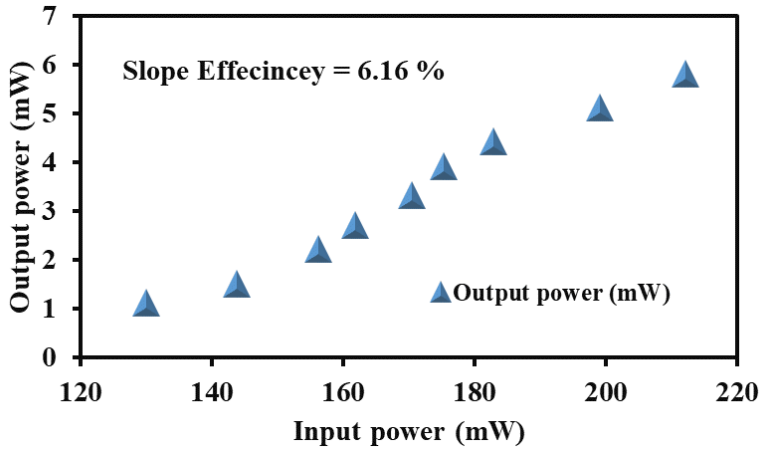


Figure 10. Output power vs. input power with a slope efficiency indicating effective energy conversion.

The illustrates the absorption properties of the fiber laser's saturable absorber at two critical wavelengths at 1557.2 nm, the absorption measures 0.78 dB. This suggests that the saturable absorber has a modest increase in absorption at longer wavelengths, characteristic of materials having wavelength-dependent characteristics, as seen in Fig. 11.

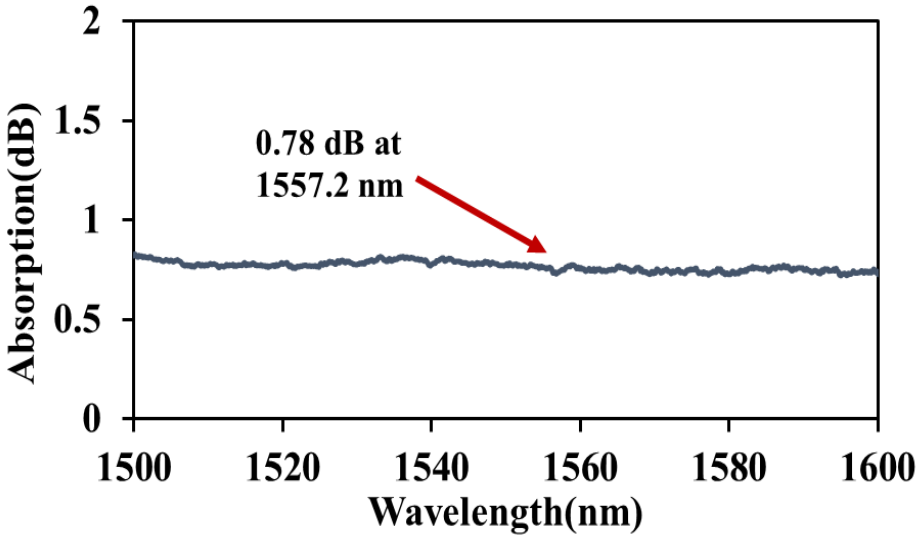


Figure 11. The linear SA absorption at 1577.2 nm

Fig. 12, illustrates the saturation absorption curve. At a saturation intensity of 80 MW/cm², the saturable absorption is measured at 4.1%, while the non-saturable absorption is recorded at 3.0%. This curve elucidates the efficacy of the saturable absorber material in regulating pulse production. The decreased non-saturable absorption indicates that the material mostly depends on saturable absorption at elevated intensities for efficient pulse shaping.

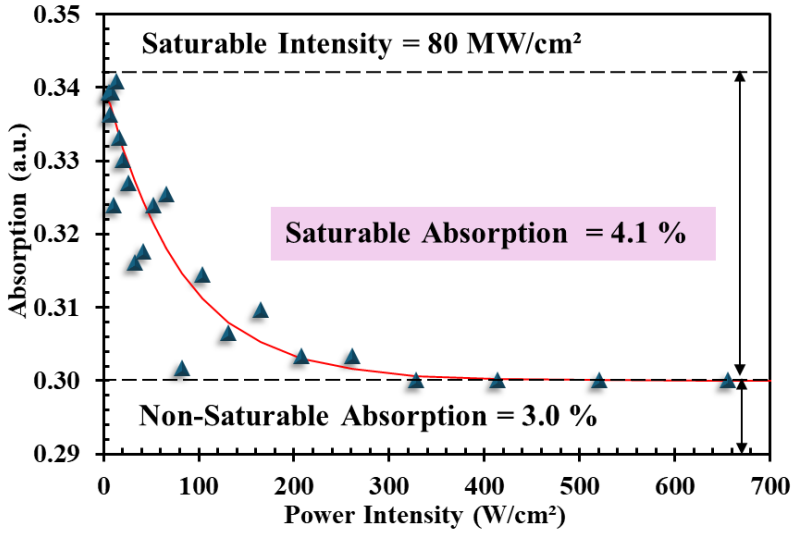


Figure 12. The nonlinear SA absorption at 1577.2 nm

Table 1 shows a comparison of the main performance parameters of Mode-locked pulse lasers that use different types of saturable absorbers. These numbers are very important for figuring out how efficient a laser is and if it is suited for particular photonic uses. The PANI–BN saturable absorber can handle more energy and has better dynamic performance than the other materials because it can operate with a wider range of pump power and higher repetition rates. PANI–BN has a good signal-to-noise ratio (SNR), which means that it has great pulse stability and works with very little noise. The parameters listed above show how promising PANI–BN is as a possible saturable absorber for advanced photonic devices, particularly for lasers that demand excellent performance and stability.

Table 1: Comparison between Mode-locked using PANI-BN- SA with other SAs.

Materials	**Pump Power (mW)**	**Operational Wavelength (nm)**	**Repetition Rate (MHz)**	**Pulse width (ns)**	**OPM (mW)**	**SNR (dB)**	**Ref**
Monolayer graphene	59 – 187	1561	1.21	209	4.8	60	**[25]**
black phosphorus	113.3 – 175.9	1572	50 – 66.1	4.04 - 2.43	0.7 – 3.47	66.1	**[26]**
Graphene	80.63 – 163.16	1558	20.8	605	-	5	**[27]**
BEDF	59.1 – 162.2	1603	14.29 – 29.69	26.52 – 14.8	2.85	52.73	**[28]**

Au-NPs	45.6	168.1	6.25	933	1.94 – 3.7	57.8	**[29]**
PANI-BN	92.7 [29]–212.1	1530.2-1557.2	1.225	1140.9	1.1 – 5.8	70	**This work**

5. Conclusion

This work illustrates the effective deployment of a dual-wavelength fiber laser using Polyaniline Boron Nitride Nanocomposite (PANI-BN) as a saturable absorber, resulting in stable mode-locked dark pulse production at 1532.4 nm and 1557.2 nm, with a spectral separation of 24.8 nm. The use of PANI-BN, a nanocomposite exhibiting distinctive nonlinear optical characteristics, enables effective pulse generation throughout a spectrum of pump powers (129.9 mW to 212.1 mW), maintaining a stable repetition rate of 1.225 MHz. The laser demonstrates changeable pulse width and energy, ranging from 559 ns to 502 ns for pulse width and from 1140.9 nJ to 216.3 nJ for pulse energy, while sustaining an average output power of 1.1 mW to 5.8 mW. The system attains a slope efficiency of 6.16%, signifying effective energy conversion. The dual-wavelength operation, including a notable 24.8 nm separation, renders this laser system appropriate for high-resolution spectroscopy, optical communications, and sensing applications. The results underscore the promise of PANI-BN nanocomposites as a viable optical modulator, paving the way for more compact, efficient, and versatile fiber laser systems. This work is significant for its contribution to the advancement of fiber laser technologies applicable in various scientific and industrial domains. Future efforts may concentrate on further optimizing the PANI-BN nanocomposite and investigating additional wavelength configurations to improve performance.

References

[1] S. Pavlova, M. E. Yagci, S. K. Eken, E. Tunckol, and I. Pavlov, "High power microsecond fiber laser at 1.5 μ m," *Optics Express,* vol. 28, no. 12, pp. 18368–18375, 2020.

[2] X. Chen *et al.*, "High-power femtosecond all-fiber laser system at 1.5 μm with a fundamental repetition rate of 4.9 GHz," *Optics Letters,* vol. 46, no. 8, pp. 1872–1875, 2021.

[3] H. S. Albaqawi, F. Hedhili, S. Chebaane, A. Meftah, and S. M. Al-Shomar, "Q-switched fiber laser generation utilizing metal oxide-based saturable absorber in the region of 1.0 μm and 1.5 μm," *Optik,* vol. 298, p. 171597, 2024.

[4] H. Ali, N. Arsad, N. Zulkipli, A. Rosol, M. Yasin, and S. Harun, "Q-switching pulse generation in multi-wavelength Brillouin Erbium-doped Fiber laser," *Optics Communications,* vol. 534, p. 129300, 2023.

[5] A. Ghosh *et al.*, "Q-switched pulse generation by stimulated Brillouin scattering assisted four-wave mixing effect in erbium–bismuth co-doped multi-elements silica glass based optical fiber laser," *Laser Physics,* vol. 33, no. 12, p. 125103, 2023.

[6] Z. Li *et al.*, "Random laser emission at 1064 and 1550 nm in a Er/Yb co-doped fiber-based dual-wavelength random fiber laser," *Optics Express,* vol. 32, no. 4, pp. 5737–5747, 2024.

[7] Z. Orhun, D. Doğan, Ü. Erdem, G. Yıldırım, Z. O. Pehlivanlı, and A. Ü. Metin, "Design of dual-conductive polyacrylonitrile-based composite nanofiber: Synergistic effect of

copper nanoparticles decorated-boron nitride and polyaniline," *Polymer Composites,* vol. 45, no. 3, pp. 2685–2700, 2024.
[8] R. N. Goswami *et al.*, "Polyaniline-wrapped h-boron nitride nanosheets as anticorrosive filler in epoxy coatings for substantially enhanced protection of mild steel," *Journal of Industrial and Engineering Chemistry,* vol. 140, pp. 285–297, 2024.
[9] M. M. Rahman *et al.*, "Synthesis of hexagonal boron nitride based PANI/h-BN and PANI-PPy/h-BN nanocomposites for efficient supercapacitors," *Journal of Alloys and Compounds,* vol. 947, p. 169471, 2023.
[10] S. Subbaiah, P. S. Muthukrishnan, R. Gurusamy, S. Venkatachalam, T. R. Rajasekaran, and N. Srinivasan, "Boron nitride/polyaniline composite-based hybrid electrode for pseudocapacitor application," *Journal of Materials Science: Materials in Electronics,* vol. 34, no. 5, p. 397, 2023.
[11] M. Li *et al.*, "Boron Nitride-Polymer Composites with High Thermal Conductivity: Preparation, Functionalization Strategy and Innovative Structural Regulation," *Small,* vol. 21, no. 20, p. 2412447, 2025.
[12] L. Shubhadarshinee, P. Mohapatra, S. Behera, B. R. Jali, P. Mohapatra, and A. K. Barick, "Review on synthesis and characterization of metal nanoparticles doped carbon nanofillers based nanohybrids reinforced polyaniline nanocomposites," *Polymer-Plastics Technology and Materials,* vol. 63, no. 8, pp. 1011–1035, 2024.
[13] J. Tao, P. Song, C. Lv, L. Hou, B. Lu, and J. Bai, "Generation of widely tunable single- and dual-wavelength in a figure-eight mode-locked fiber laser," *Optics & Laser Technology,* vol. 160, p. 109107, 2023.
[14] Q. Lu, H. Liu, C. Quan, Q. Wu, F. Zhang, and L. Hou, "Flexible dual-wavelength mode-locked fiber laser using spun fiber filter," *Journal of Lightwave Technology,* 2024.
[15] T. Li *et al.*, "Wavelength-switchable dual-wavelength thulium-doped fiber laser utilizing photonic crystal fiber," *Optics Communications,* vol. 528, p. 129033, 2023.
[16] W. Chen *et al.*, "Dual-Wavelength Fiber Laser Inscribed By Femtosecond Laser In High-Erbium-Doped Fiber," *IEEE Photonics Technology Letters,* 2025.
[17] X. Wang, Z. Wang, C. Shen, X. Zhang, S. Huang, and T. Guo, "Generation of spatiotemporal dark pulse or polarization domain wall solitons in a partial multimode mode-locked fiber laser," *Infrared Physics & Technology,* vol. 138, p. 105249, 2024.
[18] Z. Li *et al.*, "Generation of mode-locked states of conventional solitons and bright-dark solitons in graphene mode-locked fiber laser," *Frontiers of Optoelectronics,* vol. 16, no. 1, p. 12, 2023.
[19] K. Jia *et al.*, "Dark-bright pair between bright pulses in a multimodal interference-based Q-switched mode-locking fiber laser," in *Advanced Lasers, High-Power Lasers, and Applications XIV*, 2023, vol. 12760: SPIE, pp. 140–144.
[20] M. M. Fadhel, A. E. Hamzah, M. S. D. Zan, N. Abd Aziz, and N. Arsad, "Generation of stable dual-wavelength mode-locked pulses using boron nitride saturable absorber in all-polarization-maintaining Er-doped fiber laser," *Optical Materials,* vol. 157, p. 116352, 2024.
[21] S. Paul and B. Karthikeyan, "Modification of the Exciton Lifetime and Saturable Absorption Behavior of ZnO@ MoS2/Polyaniline Nanocomposite Films," *ACS Applied Optical Materials,* vol. 2, no. 5, pp. 842–851, 2024.
[22] S. Kumar M, M. Mohandas, S. Jeferson, and R. Jayavel, "Engineering Scalable and Cost-Effective Fabrication of Architecturally Tailored Boron Nitride-Epoxy-Silane-Functionalized Cardanol Nanocomposites for Advanced Microwave Absorption Applications," *Langmuir,* vol. 41, no. 7, pp. 4658–4671, 2025.
[23] M. Zhu *et al.*, "Boron nitride quantum dots-decorated ferroelectric nanofibers for high performance wearable photodetectors," *Materials Today Nano,* vol. 25, p. 100445, 2024.
[24] S. E. Kim, K. Sankar, J. C. Yoon, A. Muthurasu, and H. Y. Kim, "Integration of Carboxylate Carbon Dot-Supported Gold Nanoparticles with Boron Nitride Nanosheets for Electrochemical Sensing of Prostate-Specific Antigen via Sandwich Immunoassays," *ACS Applied Bio Materials,* vol. 8, no. 5, pp. 4153–4165, 2025.

[25] Q. Bao *et al.*, "Monolayer graphene as a saturable absorber in a mode-locked laser," *Nano Research,* vol. 4, no. 3, pp. 297–307, 2011.
[26] Z. Qin, G. Xie, C. Zhao, S. Wen, P. Yuan, and L. Qian, "Mid-infrared mode-locked pulse generation with multilayer black phosphorus as saturable absorber," *Optics Letters,* vol. 41, no. 1, pp. 56–59, 2015.
[27] X. Li, D. Wang, K. Hua, Q. Chen, Y. Ge, and Q. Xia, "Saturable absorber based on graphene for a hybrid passive mode-locked erbium-doped fiber laser," *Optical Fiber Technology,* vol. 70, p. 102867, 2022.
[28] H. Ali *et al.*, "Investigating the Impact of SMF on Brillouin Fiber Laser Performance," in *Journal of Physics: Conference Series*, 2023, vol. 2627, no. 1: IOP Publishing, p. 012007.
[29] N. Naharuddin *et al.*, "Pulsed-laser-ablated gold-nanoparticles saturable absorber for mode-locked erbium-doped fiber lasers," *Optics & Laser Technology,* vol. 150, p. 107875, 2022.